Beam Motions Near Separatrix*

M. Ball[1] B. Brabson[1] J. Budnick[1] C.M. Chu[1] D.D. Caussyn[1] J. Collins[1] V. Derenchuk[1]
G. East[1] M. Ellison[1] D. Friesel[1] K.M. Fung[1] B. Hamilton[1] W.C. Hsi[1] H. Huang[2]
W.P. Jones[1] S.Y. Lee[1] D. Li[3] K.Y. Ng[4] X. Pei[5] A. Riabko[1] and T. Sloan[1]
[1]Indiana University, Bloomington, IN 47405, [2] Brookhaven National Laboratory,
[3] Lawrence Berkeley national Laboratory, [4] Fermilab, [5] Lucent Technology.

Abstract

Experimental data on particle motion near the separatrix of the one dimensional (1-D) fourth-integer islands are analyzed. When the beam bunch is initially kicked to the separatrix orbit, we observed a strong decoherence in the coherent betatron motion. We find that, through intensive particle tracking simulation analysis, the decoherence has resulted from the beam being split into beamlets in the betatron phase space. However, we also observe an unexpected recoherence of coherence signal, which may result form a modulated closed orbit or the homoclinic structure near the separatrix.

1 INTRODUCTION

Particle motion along the separatrix is important in the stochastic slow beam extraction. Since the stochasticity layer at the separatrix orbit is further enhanced by the time dependent dipole and quadrupole modulations [1, 2], the study of particle motion near separatrix can provide needed information on the dynamical aperture and lifetime of stored beam particles. Thus it is important to study the dynamics of particle motion near the separatrix.

In our previous studies [3, 4], we studied particle motion at the fourth order resonance, and examined the effects of tune modulation on particle motion inside the island. We mapped out a boundary of stability by analyzing our experimental data on the tune modulation to the particle trapped at the center of the resonance islands. This paper studies the dynamics of particle motion near separatrix.

Although the particle motion near the separatrix is complicated by rapid decoherence and inherent finite beam size in our experiments, we can re-analyze our data to explore the effects of inherent noise for particle motion near separatrix because we have made many progresses in understanding the dynamics of particle motion near the separatrix. [2] The paper is organized as follows. Section 2 outlines our experimental setup and gives a brief review of the nonlinear Hamiltonian model. Section 3 discusses the data analysis. The conclusion is given in Sec 4.

* Work supported by U.S. Department of Energy DE-FG02-92ER40747 and National Science Foundation PHY-9512832.

2 NONLINEAR BETATRON RESONANCE AND EXPERIMENTAL METHOD

Particle motion in accelerators is governed by the linear Hill's equation, where dipoles provide a closed orbit, and quadrupoles provide linear focusing for beam stability. However, sextupole and higher multipoles are needed to correct chromatic aberration, and are inherent components in magnets. By design, the nonlinear perturbation in accelerator is small except when the nonlinear resonance condition is encountered, i.e. $m\nu_x + n\nu_z = \ell$, where m, n and ℓ are integers. This paper studies the $4\nu_x = 15$ resonance.

Near an isolated single resonance ($m\nu = \ell$, hereafter, the subscript is neglected) in the resonance rotating frame, the Hamiltonian can be approximated by [5]

$$H \approx \delta J + \frac{1}{2}\alpha J^2 + gJ^{\frac{m}{2}}\cos(m\psi), \qquad (1)$$

where J and ψ are the conjugate action-angle variables, $\delta = \nu - (\ell/m)$ is the resonance proximity parameter, ν is the betatron tune, α is the nonlinear detuning parameter arising from higher-order multipoles, and g is resonance strength. The phase ψ in the resonance rotating frame is related to the betatron phase ϕ by

$$\psi = \phi - \frac{\ell}{m}\,\theta + \frac{\chi}{m}.$$

The θ is orbit angle serving as the time coordinate and χ is the resonance phase that depends on the measurement location.

This Hamiltonian is time-independent. A torus is the Hamiltonian flow at a constant 'energy,' i.e. $H(J, \psi) = E$. Hamilton's equations of motion are

$$\begin{aligned} \dot{\psi} &= \delta + \alpha\, J + \frac{m}{2}\, g\, J^{\frac{m}{2}-1}\, \cos(m\,\psi), \\ \dot{J} &= m\, g\, J^{\frac{m}{2}} \sin(m\,\psi) \end{aligned} \qquad (2)$$

where the overdot corresponds the derivative with respect to the time coordinate θ.

2.1 Experimental setup at the IUCF Cooler Ring

The procedure of our experiments is as follows. The 90 MeV H_2^+ beam was stripped injected into the Cooler for attaining 45 MeV protons. The cycle time was 10 s. The beam was electron cooled for 3 s before we started our experiments. The cooling time was about 0.3 s. Typical, we had about 3×10^8 protons per bunch with a bunch length of about 5.4 m (or 60 ns) FWHM. The revolution period was 969 ns, and the rf cavity was operating at a frequency $f_0 = 1.03168$ MHz with the harmonic number h = 1. The 95% emittance was about $0.3\ \pi$ mm-mrad, and the stability of the horizontal close orbit was smaller than 0.05 mm FWHM. Details of our experimental setup have been published [6].

To study the nonlinear resonance at $4\nu_x = 15$, we adjusted our horizontal betatron tune to the resonance line. A ferrite kicker with the rise and fall time of about 100 ns and a flat top of about 700 ns was used to impart a transverse angular kick to the beam. The subsequent beam positions were tracked and digitized by two beam position monitors. The data $(x_1, x_2)_i$ are transformed to the normalized phase space $(x, p_x)_i$ with known betatron amplitude functions, and BPM calibrations. Figure 1 shows the Poincaré maps for some typical Hamiltonian tori with five different kicker amplitudes. The separatrix orbit is also drawn to compare our experimental data. Properties of this fourth-integer resonances have been successfully explored [3].

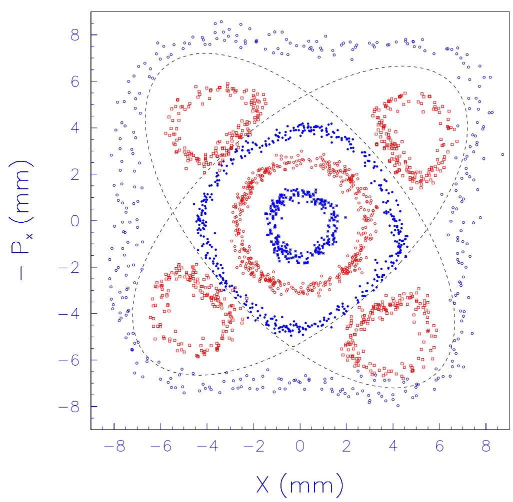

Figure 1: Poincaré map shows beam sampling the nonlinear fourth-integer resonance by exciting particles with five different kicker amplitudes, increasingly kicker amplitudes corresponding the lager radius contours. The line is the predicted separatrix. Beam motion close to separatrix is evident.

2.2 *Multiparticle Simulation Model*

Our experiments were intended to explore the single particle motion near a betatron resonance. However, the beam bunch in accelerators is composed of many particles. Because of the electron cooling, and the random noises inherent in all accelerators, the beam bunch reaches an equilibrium emittance [7]:

$$\rho(x, p_x) = C e^{-H/kT} = \frac{1}{2\,\pi\,\sigma^2}\, e^{(x^2+p_x^2)/2\,\sigma^2}, \qquad (3)$$

where C is the normalization constant, H is the Hamiltonian, "kT" is the effective thermal energy, x and p_x are the normalized conjugate phase space coordinates, and $\sigma^2 = \beta_x\, \epsilon_{rms}$ with an rms emittance ϵ_{rms}. Here, we have assumed a linear Hamiltonian at the center of the phase space.

The phase space evolution of Eq. (2) can be attained by the symplectic map:

$$\begin{aligned} \psi_{n+1} &= \psi_n + \delta + \alpha\, J_n + \frac{m}{2}\, g\, J_n^{\;\frac{m}{2}-1} \cos(m\,\psi_n), \\ J_{n+1} &= J_n + m\, g\, J_n^{\frac{m}{2}} \sin(m\,\psi_{n+1}), \end{aligned} \qquad (4)$$

which preserves the phase space area. For particle motion near the separatrix, two hundreds steps is used for each orbital revolution. Typically, 4000 test particles with a Gaussian distribution, distributed in 3 σ region of the phase space are used in our numerical simulations.

3 DATA ANALYSIS

First, we analyze Poincaré maps that are outside the resonance region and obtain a consistent set of betatron amplitude functions, and the phase difference between two BPMs. This procedure establishes the method of transforming our digitized data to the normalized phase space coordinates. Our results are shown in Fig. 1. Since the Hamiltonian of Eq. (1) is a quadratic equation, the separatrix is given by two intersecting ellipses.

The decoherent of betatron motion a beam with finite emittance can be used to determine the nonlinear detuning parameter α. Similarly, the FFT spectra and the size of the resonance islands can be used to determine the resonance proximity parameter, and the resonance strength g. These analysis provide us a self consistent set of data for the effective nonlinear Hamiltonian.

3.1 *Motion Near the Separatrix*

Figure2 shows the centroid of beam motions a 300 revolutions when the beam is kicked onto the separatrix, where solid points correspond to the first 50 revolutions. To understand the rapid decoherence, we carry out multiparticle simulations. Figure 3 shows the beam distribution after 500 revolutions for a beam with an initial emittance of 0.3 π-mm-mrad. The decoherence arises from the fact that the beam bunch splits into beamlets under the action of the separatrix. Particles inside the separatrix move in one direction, while the particles inside the resonance island are trapped. Such a rapid decoherent is very sensitive to the emittance of the beam. Our multiparticle simulations show that the beam emittance of 0.3π mm-mrad describes very well the strong decoherence.

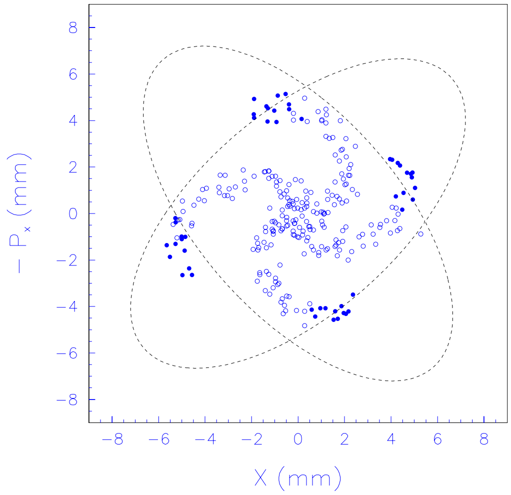

Figure 2: Poincaré map shows the data of the first 300 revolutions, where the first 50 revolutions is shown as solid points. Decoherence is due to the fact beam particles move along separatrix. The separatrix of Fig. 1 is also drawn for reference.

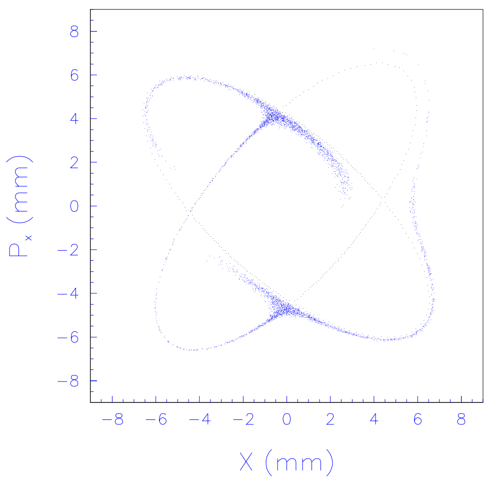

Figure 3: The plot shows the final beam distribution at 500 revolutions.

It is worth noting that our long-term experimental data shows significant recoherence of the coherent betatron motion shown in Fig. 4. Our model can not explain such a rapid recoherence, instead, it predicts a very strong recoherence at 1600 revolutions. The sizable early recoherence may arise from either closed orbit modulation of the order of 0.2 mm or the sensitivity of particle motion (homoclinic structure) near the UFP.

4 CONCLUSIONS

In conclusion, we have analyzed the data for the beam motion near the separatrix, and find that the decoherence of the beam signal arises from the beam being split at the UFP. We observe a significant recoherence in our data, that can not be explained by our model.

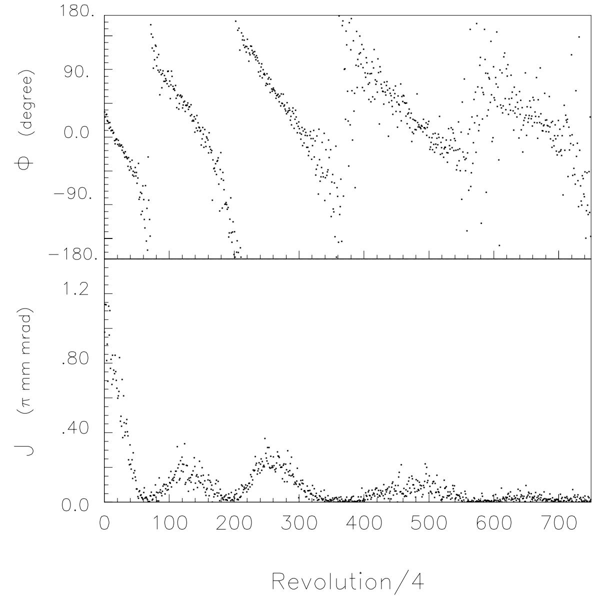

Figure 4: The rapid decoherence of coherent betatron motion in Fig. 2 is displayed in the betatron phase (top) and betatron action (bottom). Complete decoherence is observed to occurs at 240 revolutions. We note, however, that there is a significant recoherence in the coherence betatron motion at 520 and 1000 revolutions. The recoherence is associated with a phase where particles recongregate into the unstable fixed points. Numerical simulation has not been able to reproduce the recoherence of the experimental data.

In general, there are many time-dependent terms in the actual nonlinear Hamiltonian. Our model of the Hamiltonian (1) should include these terms in the simulations. The stochasticity near the separatrix orbit arises from these time dependent terms in the Hamiltonian. A more realistic numerical simulation is need for modelling the beam motion. The experimental data offer a unique challenge for the understanding of particle diffusion process in accelerators.

5 REFERENCES

[1] F. Vivaldi, Rev. Mod. Phys., **56**, 737 (1984).

[2] S.Y. Lee, *Nonlinear Beam Dynamics Experiments at IUCF Cooler Ring*, *Accelerator physics at the SSC*, AIP Proceedings No. 326, edited by Y. Yan and M. Syphers, p.13 (1995).

[3] M. Ellision et al., in *Stability of Particle Motion in Storage Rings*, AIP Conf. Proc. No 292 (AIP New York 1992), p. 170.

[4] Y. Wang et al., Phys. Rev. E **49**, 5697 (1994).

[5] S.Y. Lee, *Accelerator Physics*, (World Scientific, Singapore, 1999).

[6] S.Y. Lee et al., Phys. Rev. Lett. **67**, 3768 (1991); D.D. Caussyn et al., Phys. Rev. A **46**, 7942 (1992).

[7] M. Bai *et al.*, Phys. Rev. E**55**, 3493 (1997).